ELSEVIER

Catalysis Today 54 (1999) 119–130

CATALYSIS TODAY

www.elsevier.com/locate/cattod

The effect of operational parameters and TiO_2-doping on the photocatalytic degradation of azo-dyes

Fotini Kiriakidou, Dimitris I. Kondarides, Xenophon E. Verykios *

Department of Chemical Engineering, Institute of Chemical Engineering and High Temperature Processes, University of Patras, GR-26500 Patras, Greece

Abstract

The photocatalytic degradation of Acid Orange 7 (AO7), a non-biodegradable azo-dye, has been investigated over TiO_2 photocatalysts irradiated with a light source simulating solar light. The effect of operational parameters, i.e., dye concentration, photocatalyst content, pH of the solution and incident light energy on the degradation rate of aqueous solutions of AO7 has been examined. The effect of incorporating cations with valence higher (W^{6+}) and lower (Ca^{2+}) than the parent cation (Ti^{4+}) in the TiO_2 matrix has also been investigated. Results show that the employment of efficient photocatalysts and the selection of optimal operational parameters may lead to complete decolorization and to substantial decrease of the Chemical Oxygen Demand (COD) of the dye solutions.

Keywords: Photocatalysis; Azo-dye; Degradation; TiO_2; Doping

1. Introduction

Wastewaters produced from textile and other dyestuff industrial processes contain large quantities of organic dyes, which are difficult to degrade with standard biological methods. Within the overall category of dyestuffs, azo-dyes constitute a significant portion and probably have the least desirable consequences in terms of surrounding ecosystems. They are resistant to aerobic degradation [1,2] and under anaerobic conditions they can be reduced to potentially carcinogenic aromatic amines [3,4].

For the removal of recalcitrant organics, traditional methods like ultrafiltration, extraction, air stripping, carbon adsorption, incineration and oxidation via ozonation [5] or hydrogen peroxide [5,6] have been applied. A disadvantage of these processes is that they are non-destructive; they simply transfer the pollutant from one phase to another [7]. Over the past few years, several Advanced Oxidation Processes (AOPs) have been proposed as alternative routes for water purification [8,9]. Among them, heterogeneous photocatalysis seems to be the most attractive method for water decontamination [7,10] and the usefulness of this method for performing degradation reactions has been successfully tested for a large variety of pollutants [11–16]. The reason for the increased interest in this method is that the process can be carried out under ambient conditions and may lead to total mineralization of organic carbon to CO_2 [13,17]. Another advantage of this method is that the photocatalyst, usually TiO_2, is inexpensive and can be supported on suitable materials [18–22].

Heterogeneous photocatalysis is based on the irradiation of a photocatalyst, usually a semiconductor such as TiO_2, with light energy equal to or greater than the band gap energy. This causes a valence-band electron to be excited to the conduction band, causing charge separation. The conduction band electrons

* Corresponding author. Fax: +30-61-991527
E-mail address: verykios@iceht.forth.gr (X.E. Verykios)

0920-5861/99/$ – see front matter
PII: S0920-5861(99)00174-1

and valence band holes can then migrate to the surface and participate in interfacial oxidation–reduction reactions. The oxidative degradation of an organic pollutant is attributed to indirect reaction at the positive hole where adsorbed water or hydroxyl groups are oxidized to hydroxyl radicals ($^{\bullet}$OH), which then react with the pollutant molecule [23].

In cases where colored organic compounds exist, the color may, after adsorption onto the semiconducting surfaces, be promoted to an excited state following interaction with visible radiation and thus act as a photosensitiser [24,25]. The degradation of the colored substance may then take place through electron injection into the conduction band of the semiconductor and subsequent oxidation of the cation radical. This process is called sensitized photocatalysis. The sensitized photocatalytic process is advantageous because it extends the range of excitation energies into the visible range, making fuller use of solar energy. Similar products are created at direct and sensitized photocatalysis, and these appear to involve primarily oxidative steps when oxygen is present in the system [24].

The aim of the present study is to investigate the photocatalytic degradation of azo-dyes over semiconductive, TiO_2-based, photocatalysts irradiated with a source simulating the solar spectrum (Xe-arc lamp). The effects of doping of TiO_2 as well as the effects of operational parameters, such as dye concentration, pH of the solution and incident photon energy, on the degradation rate of aqueous dye solutions is examined. It is shown that incorporation of cations of valence higher than the parent cation (W^{6+}) into the crystal matrix of TiO_2 results in enhanced degradation rates while the opposite is observed upon doping with cations of lower valence (Ca^{2+}). It is concluded that the employment of efficient photocatalysts and the selection of optimal operating conditions may lead to complete decolorization and to substantial decrease of the Chemical Oxygen Demand (COD) of the dye solutions.

2. Experimental

2.1. Materials

The semiconductor employed as photocatalyst was commercial TiO_2 (Degussa P25), in powder form, and was used as received. According to the manufacturer, P25 has a primary particle size of 40 μm, a specific surface area of $50 \pm 15\ m^2/g$ and its crystalline mode is 20% rutile and 80% anatase.

Acid Orange 7 (AO7, Aldrich) has been chosen as a representative model compound. AO7 is a non-biodegradable synthetic azo-dye, with a molecular formula of $C_{16}H_{11}N_2O_4SNa$, widely used in the textile industry.

2.2. Preparation of doped TiO_2 photocatalysts

The influence of altervalent cation doping of TiO_2 on its photocatalytic performance for the degradation of AO7 was investigated by incorporating cations of lower (Ca^{2+}) and higher (W^{6+}) valence than that of the host cation (Ti^{4+}) into the matrix of TiO_2. A series of TiO_2 photocatalysts doped with 0.22–0.67 at.% of W^{6+}, and with 0.20–0.95 at.% of Ca^{2+} have been prepared. In the continue, these samples will be denoted as TiO_2(x% D), where D indicates the dopant cation of concentration x (at.%).

Precursors used for the preparation of W^{6+}-and Ca^{2+}-doped TiO_2 photocatalysts were $(NH_4)_{12}W_{12}O_{41}\cdot 5H_2O$ and CaO, respectively, obtained from Alfa Products.

For the preparation of W^{6+}-doped TiO_2, an appropriate amount of ammonium tungstate, calculated to give the desired dopant concentration in the final material, was added in water at pH 14 (pH adjusted with NH_3). The solution was then heated at 70°C under continuous stirring to achieve complete dissolution of the salt. An appropriate amount of TiO_2, dispersed in distilled water, was then added to the solution and the mixture was heated gently to 80°C. The slurry was maintained at this temperature until nearly all the water evaporated and the solid residue was subsequently calcined in air at 900°C for 5 h. Calcination temperature was approached with a heating rate of 3°C/min, while cooling of the material was done slowly, with a rate of approximately 10°C/min.

Ca^{2+}-doped TiO_2 samples were prepared in a similar manner. Appropriate amounts of CaO and TiO_2 powders were dispersed in distilled water and thoroughly mixed. The procedures of evaporation of water and of calcination at 900°C were identical as in the case of the W^{6+}-doped TiO_2. A reference (undoped)

TiO_2 photocatalyst was also prepared following this method, but was calcined at 700 instead of 900°C.

2.3. Experimental procedures and techniques

The experimental apparatus employed for the investigation of the photocatalytic degradation of AO7 has been described in detail elsewhere [26,28]. It consists of an illumination source, the photoreactor and the analysis system. The light source (Oriel, model 66021) is furnished with solar-light simulating Xe-arc lamp (Osram XBO 450W), a set of lenses for light collection and focusing, and a water filter mounted on the lamp housing to eliminate infrared radiation. The quartz photoreactor is equipped with optical flat light entry and exit windows and a top cover with provisions for gas inlet and outlet and for sample removal from the gas-and liquid phase. The photocatalyst particles are maintained in suspension by stirring and air bubbling. A double-bundled UV/vis spectrophotometer (Hitachi, Model U 2001) with 10 mm quartz cuvettes was used for the determination of the dye concentrations in the samples.

In a typical experiment, a known amount of AO7 is dissolved in 70 ml of distilled water in the photoreactor. The photocatalyst is then added under continuous stirring and an air flow of 60 cc/min is permitted to enter the photoreactor. After 15 min in the dark, light is allowed to irradiate the suspension and the first sample is taken ($t = 0$). For all experiments reported here, the lamp power was kept constant at 400 W. During the experiment (about 8 h) 1 ml-samples are taken from the suspension for analysis at appropriate time intervals. The photocatalyst is immediately removed from the samples after centrifugation and filtration with a syringe filter (0.2 μm, Gelman Sciences, 4192). Part of the sample is used for the measurements on the spectrophotometer (UV/vis) and, in certain cases, the rest is used for measuring COD. The concentration of AO7 in each sample is calculated using calibration curves at 485 nm. The COD is measured with standard methods.

The capacity of TiO_2 (P25) toward AO7 adsorption was measured at pH 2, 6 and 12, as a function of initial dye concentration in the solution. For each pH value, equal amounts of TiO_2(20 mg) were placed in a series of test tubes into which 10 ml of AO7 solutions with variable dye concentrations (C_i) was added. The samples were then left overnight in the dark, in order for the dye to adsorb onto the catalyst surface, and then filtered. The extent of the equilibrium adsorption was determined from the decrease in the dye concentrations (ΔC_i) detected after filtration. The pH of the solution was adjusted using either HNO_3 (pH 2) or NaOH (pH 12). It should be noted that some differences in adsorption capacity might exist under irradiation. However, there is no simple experimental technique to estimate uptakes under photoreaction conditions.

All photocatalyst samples have been characterized in terms of their specific surface area and percentage of anatase to rutile form employing the BET and XRD techniques.

3. Results

The effect of operational parameters, including pH of the solution, dye concentration, photocatalyst content, incident light energy as well as of altervalent cation doping of TiO_2 was examined using the apparatus and following the procedures described above.

3.1. Catalyst characterization

The specific surface areas of the photocatalysts examined are listed in Table 1. It is observed that calcination of the undoped catalyst at 700°C results in a significant loss of surface area which decreases from 50 m^2/g (P25) to 13 m^2/g. However, doping TiO_2 with W^{6+} cations reduces the loss of surface area in a manner which depends on dopant concentration, i.e., increasing W^{6+}concentration leads to materials with increased surface areas (Table 1), even if these samples were calcined at a higher temperature (900°C). Apart from the effect on surface area, high temperature calcination also strongly influences the crystalline mode of TiO_2, which is completely transformed to its rutile form (Table 1).

Previous investigations in this laboratory have shown that high temperature calcination of the doped materials, results in the diffusion of the dopant cations into the crystal matrix of TiO_2. This has been demonstrated by measurements of the electrical conductivity and activation energy of electron conduction of the

Table 1
Specific surface areas and crystalline mode of the doped and undoped catalysts examined

Photocatalyst description	Surface area (m^2/g)	Crystalline mode (% rutile)
TiO_2, Degussa P25	50	20
TiO_2 (calcined at 700°C)	13.0	100
TiO_2 (0.22% W^{6+})	10	100
TiO_2 (0.34% W^{6+})	10.5	100
TiO_2 (0.45% W^{6+})	14.5	100
TiO_2 (0.56% W^{6+})	15	100
TiO_2 (0.67% W^{6+})	16.5	100
TiO_2 (0.20% Ca^{2+})	6	100
TiO_2 (0.95% Ca^{2+})	6.5	100

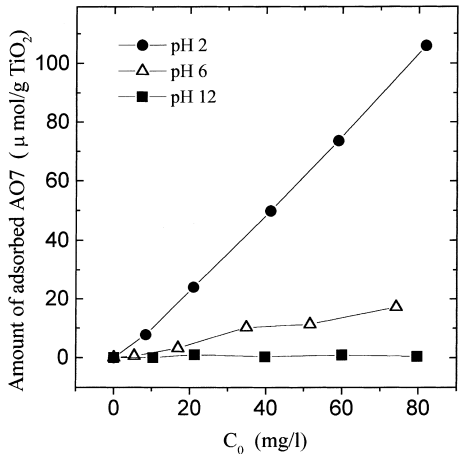

Fig. 1. Capacity of TiO_2 (P25) toward AO7 adsorption, as a function of initial dye concentration, at pH of the solution equal to 2, 6 (natural) and 12, T_{ad}: 25°C; dark conditions.

doped materials [29,30]. This diffusion process, which results in replacement of the parent Ti^{4+} cations with dopant cations, is probably responsible for the preservation of surface area observed for the doped samples.

Adsorption of AO7 on TiO_2 (P25) has been investigated by measuring the capacity of the photocatalyst toward AO7 adsorption at 25°C, following the procedure described in a previous paragraph. Preliminary experiments showed that the dye adsorbs onto the TiO_2 surface from aqueous solutions in a way which strongly depends on the pH of the solution. In order to examine this, the adsorption capacity of TiO_2 (P25) was measured at pH 2, 6 (natural) and 12. Results are shown in Fig. 1, where the amount of dye adsorbed per gram of TiO_2 is plotted as a function of the initial dye concentration. It is observed that the amount of AO7 adsorbed at pH 12 is negligible while a large amount of AO7 is adsorbed at pH 2. At pH 6 an intermediate amount of dye is adsorbed.

3.2. Effect of operational parameters on the photocatalytic degradation of AO7

The effect of experimental parameters on the photocatalytic degradation of AO7 was investigated employing TiO_2 (P25) as photocatalyst. The effect of the pH of the solution on the decolorization of AO7 solutions has been examined in the pH range of 2–12 and the results are presented in Fig. 2. The degradation curves of AO7 are presented as the time-dependent normalized dye concentration, which is the dye concentration remaining at any time divided by the initial

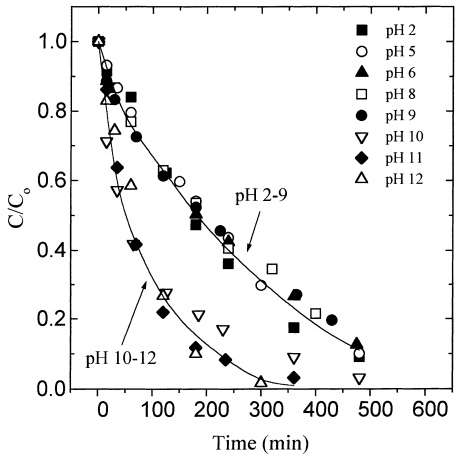

Fig. 2. Effect of the initial pH on the decolorization of aqueous solutions of AO7, C_0: 300 mg/l; C_{TiO2}: 0.75 g/l.

dye concentration (C/C_0). It is observed that the corresponding curves fall into two distinct regions: one for pH 2–9 and one for pH 10–12. It is obvious that photodegradation of AO7 is strongly favored at pH greater than 10 (basic solutions), where complete decolorization occurs in less than 6 h, while at pH lower than 9 the degradation is much slower and more than 8 h are needed for complete degradation of the dye. Because of the significant differences observed in the degradation rate of AO7 at basic and neutral (or acidic) solutions, experiments presented in the following sections were obtained for both pH 6 and 12.

The influence of the initial dye concentration on the decolorisation of AO7 at pH 6 and 12 is presented in Fig. 3(A, B) respectively, where the normalized concentration of AO7 in the solution is plotted as a function of time of irradiation, for each experiment. The initial AO7 concentration was varied between 25 and 600 mg/l for the experiments conducted at pH 6 and between 25 and 1000 mg/l for those conducted at pH 12. It is clearly observed that the time required for the decolorization of AO7 solutions at both pH 6 and 12 depend significantly on the initial dye concentration. At pH 6 (Fig. 3(A)), complete decolorization of the solutions takes place in less than an hour for relatively low C_0 values (25–100 mg/l) while this is not the case for higher initial dye concentrations (200–600 mg/l). On the other hand, degradation of AO7 at basic solutions (Fig. 3(B)) is much faster and complete decolorization occurs even at $C_0 = 600$ mg/l, in less than 4.5 h.

Comparison of the degradation curves obtained at pH 6 (Fig. 3(A)) and 12 (Fig. 3(B)) clearly shows that, in all cases, the photoreaction is much faster at basic solutions. It is also worth noting that the degradation of AO7 at pH 6 can be fitted by first order kinetics (exponential lines in Fig. 3(A)), while that at pH 12 can be fitted by zero order kinetics (straight lines in Fig. 3(B)). The initial reaction rates (per gram of catalyst) calculated from the fitted lines of Fig. 3 are presented in Fig. 4, where the initial decolorization rates obtained at pH 6 and 12 are plotted as a function of initial dye concentration. At pH 6, a relatively constant initial rate is observed for $C_0 = 25$–100 mg/l while further increase in the initial dye concentration leads to decreased initial degradation rates (Fig. 4). The same behavior is observed at pH 12 but the initial rate is constant for a wider range of initial dye concentrations

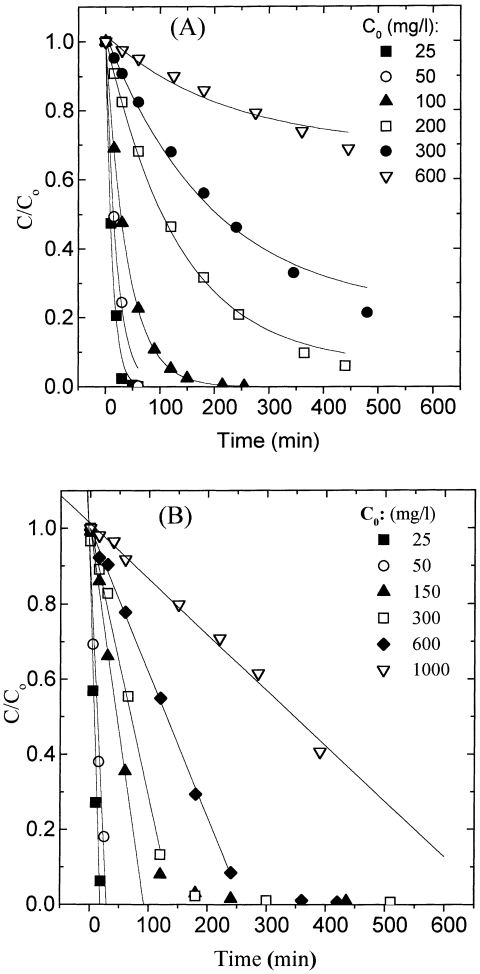

Fig. 3. Effect of the initial dye concentration on the decolorization of aqueous solutions of AO7 at pH 6 (A) and 12 (B), C_{TiO2}: 0.75 g/l.

(25–600 mg/l). The initial rate decreases only for dye concentrations as high as 1000 mg/l (Fig. 4).

To investigate the effect of catalyst loading on degradation rate of AO7, two sets of experiments were conducted, at pH 6 and 12, employing commercial TiO_2 (Degussa P-25), in which the photocatalyst loading in the dispersion was varied between 0.37 and 4.00 g/l. Results obtained at pH 6 are presented in Fig. 5. It is observed that the irradiation time required for decolorization of the azo-dye solutions decreases with increasing catalyst loading, until a plateau is reached at concentrations above 2.0 g/l. Identical results (not shown) were obtained at pH 12. The initial rates, per

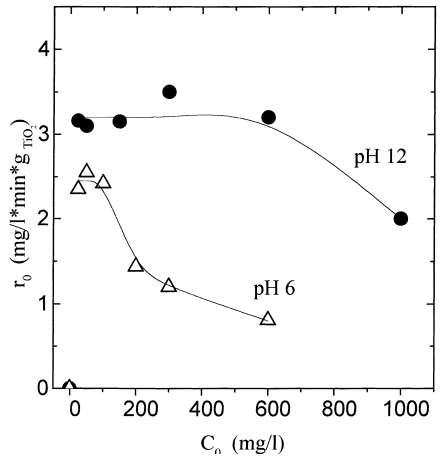

Fig. 4. Effect of the initial dye concentration on the initial degradation rate (per gram of photocatalyst) of AO7 at pH 6 and 12. Data obtained from Fig. 3.

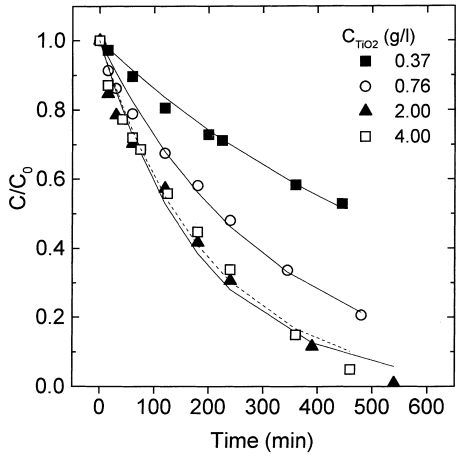

Fig. 5. Effect of the photocatalyst (TiO_2, P25) concentration on the decolorization of aqueous solutions of AO7 at pH 6, C_0: 300 mg/l.

gram of TiO_2, calculated from the degradation curves at pH 6 (Fig. 5) and pH 12, are plotted in Fig. 6 as a function of the photocatalyst concentration in the dispersion. It is observed that the initial degradation rate decreases monotonically with increasing TiO_2 content. This is more pronounced at pH 12 (Fig. 6).

In all experiments presented above, the full range of photons (except IR) emitted from the solar light simulating source was used, which consists of photons with energy higher and lower than the band gap energy of the semiconductor. To investigate the influence of the incident photon energy on the degradation rate of AO7, an experiment was conducted in which only visible light was permitted into the photoreactor. This was achieved by the use of a filter which cuts-off ultra violet radiation ($\lambda < 400$ nm). Results obtained are presented in Fig. 7, where the effect of the spectral range of incident radiation on the AO7 degradation is presented. In this Figure, the normalized dye

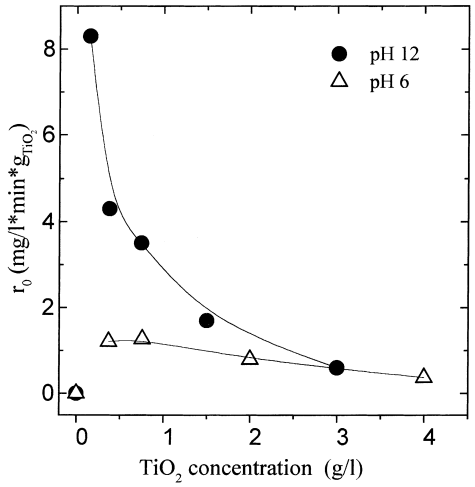

Fig. 6. Effect of the photocatalyst concentration on the initial degradation rate (per gram of TiO_2) of AO7 at pH 6 and 12.

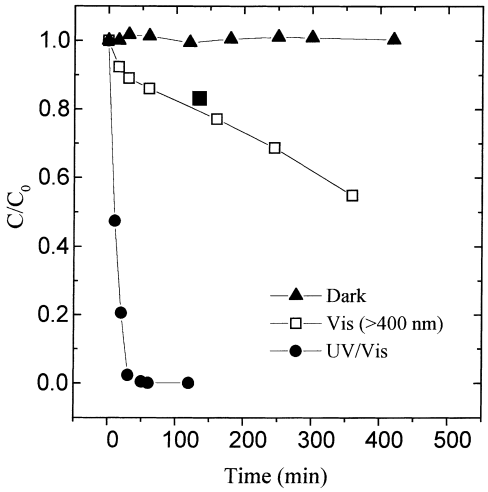

Fig. 7. Effect of the incident photon energy on the decolorization of aqueous solutions of AO7, C_0: 25 mg/l; C_{TiO2}: 0.75 g/l; pH 6.

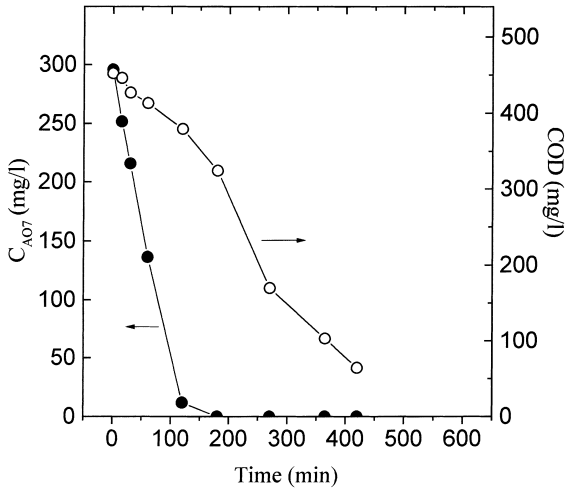

Fig. 8. Degradation of AO7 and COD removal as a function of time of illumination, C_0: 300 mg/l; C_{TiO2}: 0.75 g/l; pH 12.

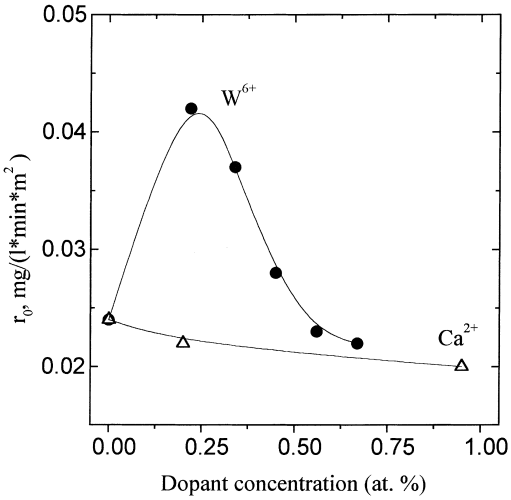

Fig. 9. Effect of dopant type and concentration on the initial degradation rate of AO7, C_0: 100 mg/l; C_{TiO2}: 0.75 g/l; pH 12.

concentration is plotted as a function of irradiation time in experiments conducted (i) using full range radiation emitted from the source (UV + vis), (ii) using only visible radiation ($\lambda < 400$ nm) and (iii) under dark conditions. It is observed that no decolorization of the solution is achieved in the absence of light, indicating that the decolorization process is photo-induced. It is obvious that the fastest degradation is achieved by using radiation which contains both UV and visible light, where complete disappearance of AO7 is achieved already after about 30 min of irradiation. When only visible light is used, AO7 degradation takes place at a much lower rate. It should be noted here that blank experiments conducted in the presence of UV/vis radiation, but in the absence of photocatalyst, did not result in any measurable degradation of AO7 (results not shown).

The results of the experiments presented in the previous paragraphs show that the decolorization rate of AO7 with photocatalytic methods is feasible. However, from the practical point of view, not only decolorization but also COD removal is of interest. In Fig. 8 are presented the AO7 concentration and the COD of the solution as functions of time of illumination, at pH 12. It should be noted here that the initial AO7 concentration in this experiment was 300 mg/l, which corresponds to a COD value of 485 mg O_2/l, while the measured COD was approximately 450 mg/l. This is due to the appreciable experimental error in the usual methods of COD measurement. As observed in Fig. 8, there is a substantial decrease of the COD of the solution, which continuously decreases with time. COD is decreased to 50% after ca 4 h, while at the end of the experiment (8 h) more than 85% of the COD is removed. However, the rate of COD removal is much lower than that of decolorization, which is completed after 2 h of illumination (Fig. 8).

3.3. Effect of altervalent cation doping of TiO_2 on the degradation rate of AO7

The effect of altervalent cation doping of TiO_2 on the decolorization rate of AO7 is presented in Fig. 9. It should be noted here that TiO_2 calcined at 700°C and not P25 is used as a reference photocatalyst in these experiments. This is due to the significant difference in particle size of these samples. The initial rate of AO7 degradation is shown in Fig. 9 as a function of dopant concentration, for dopants of lower (Ca^{2+}) and higher (W^{6+}) valence than that of the host cation (Ti^{4+}). It is observed that, upon increasing W^{6+} concentration, the decolorization rate initially increases, goes through a maximum for photocatalysts containing 0.22% W^{6+}, and then decreases for higher dopant concentrations. On the other hand, doping with Ca^{2+} results in a small decrease of the decolorization rate (Fig. 9).

4. Discussion

4.1. Effect of the pH of the solution on the adsorptive properties of TiO_2

AO7 is known to adsorb on TiO_2 particles from aqueous solutions [25]. The strong dependence of the capacity of TiO_2 towards AO7 adsorption on the pH of the solution can be explained by taking into account the intrinsic amphoteric behavior of suspended TiO_2 particles and the acidic nature of the dye. It is known that metal oxide particles suspended in water behave similar to diprotic acids. For TiO_2, hydroxyl groups undergo the following acid–base equilibria [10]:

$$> TiOH_2^{+} \overset{pK_{a1}}{\leftrightarrow} > TiOH + H^{+} \quad (1)$$

$$> TiOH \overset{pK_{a2}}{\leftrightarrow} > TiO^{-} + H^{+} \quad (2)$$

where '>TiOH' represents the 'titanol' surface group and pK_{a1}, pK_{a2} are the negative logs of the acidity constants for the first (Eq. (1)) and second (Eq. (2)) acid dissociation, respectively. For Degussa P25, $pK_{a1} = 4.5$ and $pK_{a2} = 8.0$, which yield a pH of zero point of charge equal to $pH_{zpc} = 6.25$ [10].

From the above, it is reasonable to expect that adsorption on TiO_2 will depend on the electrical charge of the dye and the photocatalyst surface. AO7 has a negatively charged sulfonic group and it is expected that, at low pH, attractive forces between the TiO_2 surface and the dye will favor adsorption. On the other hand, at high pH, the TiO_2 surface is negatively charged and repulsive forces will lead to decreased adsorption. Finally, at pH values close to the pH_{zpc}, adsorption is expected to take intermediate values.

The experimentally observed dependence of the adsorption capacity of TiO_2 towards AO7 on the pH of the solution (Fig. 1) is in agreement with the explanation given above, since the pH of the solution affects the electrical properties of the TiO_2 surface.

4.2. Effect of operational parameters on the degradation rate of AO7

4.2.1. Effect of the pH of the solution

The results presented in Fig. 2 clearly show that there is a strong dependence of the pH of the solution on the degradation rate of AO7. Although the degradation rate is rather insensitive in the pH range of 2–9, it increases significantly upon increasing pH of the solution above 10 (Fig. 2). This probably has to do with the pH-dependence of the chemisorptive properties of TiO_2, as discussed above. At $pH < 9$ ($pH < pK_{a2}$), the adsorption of AO7 is favored by the electrical nature of TiO_2. This is confirmed by the adsorption capacity curves presented in Fig. 1. It is possible that this leads to the formation of several layers of adsorbed dye on the photocatalyst surface. It is then expected that most of the adsorbed dye molecules are not in direct contact with the photocatalyst surface resulting in decreased degradation rates with decreased pH. This issue will be also discussed in the continue.

It is also possible that the observed effect of the pH on the degradation rate of AO7 is due to different photoreaction mechanisms operable at different pH. Assuming that degradation proceeds via hydroxyl radical attack, it is expected that this mechanism would be favored at $pH > pK_{a2}$, where the TiO_2 surface is highly hydroxylated. Further evidence for the operation of different photoreaction mechanisms at different pH values is given by the fact that, under all experimental conditions examined, the apparent order of the reaction is different for pH 6 (first-order, Fig. 3(A)) and pH 12 (zero-order, Fig. 3(B)). However, this issue needs further investigation. Experiments are now in progress in order to identify the intermediate products of the degradation of AO7. If more oxygenated compounds are produced at pH 12 compared to pH 6, then the mechanism involving hydroxyl radical attack is probably responsible for the observed differences.

4.2.2. Effect of initial AO7 concentration

Results presented in Fig. 3(A, B) clearly show that the time required for complete decolorization of aqueous solutions of AO7 strongly depends on the initial concentration of the dye. It is important to note that for dye concentrations below 50 mg/l, which are typically observed at wastewaters of dyehouses, complete degradation of AO7 takes place in the order of minutes, for both neutral (Fig. 3(A)) and basic (Fig. 3(B)) solutions.

Although the time required for complete decolorization of AO7 solutions increases with increasing initial dye concentration, this is not the case for the observed initial rate of the reaction (Fig. 4). For pH 6, the appar-

ent initial reaction rate remains constant with increasing initial dye concentration from 25 to 100 mg/l. Further increase of C_0 results in a progressive decrease of r_0 (Fig. 4). This dependence could again be related to the formation of several monolayers of adsorbed dye on the TiO_2 surface, which is favored at high dye concentrations, as discussed above. At $C_0 < 100$ mg/l, the surface is not completely covered leading to constant reaction rates. At higher dye concentrations, larger amounts of the dye adsorb on the photocatalyst (see adsorption isotherms of Fig. 1) and inhibit the reaction of adsorbed molecules with the photoinduced positive holes or hydroxyl radicals, since there is not a direct contact of the semiconductor with them. This results in the observed decrease in the apparent reaction rate. In addition, it should be taken into account that the incident photons can be absorbed either by the TiO_2 or by AO7 molecules present in the solution. Increasing dye concentration leads to an increase of the amount of photons which are absorbed by the dye molecules and never reach the photocatalyst surface.

On the contrary, at pH 12 where adsorption of AO7 on the photocatalyst surface is negligible (Fig. 1), there are no multilayers formed and the apparent reaction rate is relatively constant over a wide range of initial dye concentrations (25–600 mg/l, Fig. 4). Dye concentrations as high as 1000 mg/l are then required to observe a decrease in r_0 (Fig. 4).

4.2.3. Effect of photocatalyst content

The degradation curves presented in Fig. 5, show that the time required for the decolorization of aqueous solutions of AO7 decreases with increasing the photocatalyst content in the dispersion up to ca. 2.0 g/l. However, for catalyst contents above 2.0 g/l there are not significant changes. As observed in Fig. 6, the apparent initial rates per gram of catalyst decrease with increasing TiO_2 content, which is more pronounced at pH 12. This behavior is due to the so called 'shielding effect' caused by the suspended TiO_2 layers located closer to the radiation source, which reduce the penetration of light. Obviously, the shielding effect becomes more pronounced as the photocatalyst concentration increases.

A similar behavior has been observed in the study of photocatalytic cleavage of water, where the normalized intensity, I/I_0 (measured intensity at the reactor cell outlet divided by the intensity at the same point at zero catalyst loading) was examined as a function of catalyst loading. It was concluded that the reduction in the rate of H_2 production (per gram of catalyst) was due to reduced transparency of the reaction slurry caused by increased concentration of photocatalyst particles [26].

4.3. Effect of the incident photon energy

Results discussed so far clearly indicate the applicability of the photocatalytic method for the degradation of aqueous solutions of AO7 under illumination with photons having energy in the region of UV/vis radiation. Under these conditions, the process is quite fast, especially for low initial dye concentrations. This is the case for the experiment presented in Fig. 7, where complete decolorization of an AO7 solution with $C_0 = 25$ mg/l takes place in a few minutes when illuminated with UV/vis radiation. Under identical experimental conditions but in the dark, there is no change in the concentration of the dye with time, indicating that the observed changes are due to a photo-induced process. In addition, blank experiments conducted in the presence of UV/vis radiation but in the absence of photocatalyst did not result in any measurable degradation of AO7. This clearly shows that homogeneous photochemical processes do not occur under the present experimental conditions.

When a filter which cuts-off UV light is used and only visible light is permitted into the reactor ($\lambda > 400$ nm), AO7 degradation takes place at smaller but appreciable rate (Fig. 7). This indicates that in the system examined here, the mechanism involving photosensitized electron injection is also operable. According to the mechanism of sensitized photocatalysis, no charge separation is involved in the semiconductor, as in the case of direct photocatalysis. Charge injection is rather entailed from an excited state of the dye into the conduction band of the TiO_2 [27]:

$$\text{Dye} + h\nu \rightarrow {}^1\text{Dye}^* \text{ (or } {}^3\text{Dye}^*) \quad (3)$$

$${}^1\text{Dye}^* (\text{or } {}^3\text{Dye}^*) + \text{TiO}_2 \rightarrow \text{Dye}^{\bullet +} + \text{TiO}_2(\text{e}^-) \quad (4)$$

The electron injected into the TiO_2 is normally trapped by an oxygen molecule. The cation radical produced by charge injection is less stable than the ground state of the compound, but it is also extremely

susceptible to recombination if the injected electrons accumulate in the conduction band [3]. Unless the cation radical undergoes recombination, it quickly degrades to yield stable products:

$$Dye^{\bullet +} \rightarrow \text{products} \quad (5)$$

$$Dye^{\bullet +} + O_2^{\bullet -} \rightarrow \text{products} \quad (6)$$

The advantage of sensitized photocatalysis is that the range of excitation energies is extended into the visible region, as in the present case, making the use of solar light for destruction of non-biodegradable wastewaters more efficient.

4.3.1. COD removal

The results presented in Fig. 8 show that the photocatalytic process leads, apart from decolorization, to a substantial decrease of the COD of the solution. It is observed, however, that this decrease is much slower than the degradation of AO7 since the COD curve lags the dye concentration curve considerably. This is due to the formation of smaller uncolored products, during the degradation of AO7, which continue to contribute to the COD of the solution. To achieve complete degradation of the smaller organic compounds, longer irradiation time is required. Preliminary experiments showed that the intermediates formed during the photocatalytic degradation of AO7 are biodegradable and, therefore, standard biological methods could be used in combination with photocatalytic processes, for the complete mineralization of azo-dyes present in wastewaters.

4.4. Effect of altervalent cation doping on the degradation rate of AO7

The results presented in Fig. 9 clearly show that doping of TiO_2 with small amounts of cations of valence higher than Ti^{4+} results in an increase of the initial rate of the degradation of AO7, while the opposite is true upon doping with cations of valence lower than that of the host cation. The promoting effect of WO_3 addition on TiO_2 has been also reported for the photocatalytic degradation of 1,4-dichlorobenzene [31] over photocatalysts prepared by incipient wetness impregnation, followed by heat treatment, and by flame hydrolysis techniques [31,32].

Concerning the volcano-type dependence of the degradation rate of AO7 on increasing W^{6+}-dopant concentration (Fig. 9), a similar behavior has been also observed in the case of the rate of H_2 production during photocatalytic cleavage of water [28]. This behavior can be related with the dopant-induced alterations on the light-absorption capacity of $TiO_2(W^{6+})$ photocatalysts. It has been shown, using Diffuse Reflectance Spectroscopy (DRS), that light-absorption capacity of the W^{6+}-doped materials increases monotonically with increasing dopant concentration, but, at the same time, a shift of absorption bands to lower wavelengths occurs [28]. The volcano-type curve of Fig. 9 may then be attributed to the contradicting effect of these parameters on the photocatalytic activity of the W^{6+}-doped catalysts.

One would argue that the observed differences of the reaction rates with altervalent cation doping of TiO_2 are due to the morphological and/or structural changes induced by the dopants. However, the doped photocatalysts employed have similar surface areas and TiO_2 is in the rutile form in all cases (Table 1). In addition, the particle size of all photocatalysts was the same and the experiments were conducted under identical conditions. Therefore, the differences of the photocatalytic activity observed in Fig. 9, may be safely attributed to the effects induced by altervalent doping of TiO_2 on its bulk electronic structure (position of Fermi energy level, formation of new energy levels by interaction of an interstitial dopant with the semiconductor lattice, electron conductivity in the bulk semiconductor) and surface properties (thickness of the space charge layer, existence and concentration of surface states, decomposition potentials affecting the photo corrosion process) [28].

Doping of TiO_2 with cations of valence higher than that of the parent Ti^{4+} cation results in increased concentration of electrons in the conduction band, as illustrated by the following defect site reaction:

$$WO_3 \leftrightarrow W[Ti]^{2+} + TiO_2 + \tfrac{1}{2}O_2 + 2e^- \quad (7)$$

An upward shift of the Fermi energy level is also expected, and, consequently, a cathodic shift of the flat band potential, towards negative value with respect to the NHE potential. As the n-dopant concentration increases the surface barrier becomes higher and the space charge region narrower. The electron-hole pairs photogenerated within this region are efficiently

separated by the large electric field traversing the barrier, before having the chance to recombine [28].

When TiO_2 is doped with lower valence cations the opposite behavior is expected. In this case, doping results in increased concentration of holes in the valence band, as illustrated by the following defect site reaction:

$$CaO + \tfrac{1}{2}O_2(g) + 2e^- \leftrightarrow Ca[Ti]^{2-} + TiO_2 \qquad (8)$$

Furthermore, the Fermi level is shifted to lower values. This shift affects the position of the flat-band potential of TiO_2, which is shifted anodically, towards positive values with respect to the NHE potential. As the p-dopant concentration is increased, the surface barrier is lowered and the space charge region becomes progressively thicker. The transient time across the barrier is increased and the probability of the carriers recombination is enhanced, thus leading to decreased photoreaction rates [28].

5. Conclusions

Photocatalytic processes with the use of solar radiation and TiO_2-based photocatalysts can be efficiently applied for the degradation of non-biodegradable azo-dyes. Complete decolorization of aqueous solutions of Acid Orange 7 (AO7) and substantial reduction of COD can be achieved with satisfactory rates with the use of optimal operational parameters. Altervalent cation doping of TiO_2 appears to be a promising method for the development of photocatalysts with improved efficiency, as has been also shown in the case of the photocatalytic cleavage of water for hydrogen production [26,28]. In particular, the following conclusions can be drawn from the results of the present study:

1. The capacity of TiO_2 towards adsorption of AO7 strongly depends on the pH of the solution: At basic solutions adsorption is negligible, while at acidic solutions large amounts of the dye are adsorbed. At natural pH adsorption takes intermediate values.
2. Degradation of AO7 is much faster at basic solutions compared with neutral and acidic.
3. When only visible light is used (>400 nm), degradation of AO7 takes place with a low but appreciable rate, indicating that the mechanism involving photosensitized electron injection is also operable in this system, leading to charge separation with light of less than band energy.
4. Decolorization of aqueous solutions of AO7 is much faster than COD removal due to the formation of uncolored intermediate fragments. Complete mineralization is achievable under prolonged exposures.
5. The photodegradation rate of AO7 can be altered to the desired direction by altervalent cation doping of TiO_2 in a manner which depends on the valence and the concentration of the dopant. Doping TiO_2 with W^{6+} cations (0.22 at.%) results in a two-fold increase of the apparent initial degradation rate while doping with Ca^{2+} results in a small decrease of the degradation rate of AO7.

References

[1] U. Pagga, D. Brown, Chemosphere 15 (1986) 476.
[2] D. Brown, P. Laboureur, Chemosphere 12 (1983) 394.
[3] K.-T. Chung, C.E. Cerniglia, Mutat. Res. 277 (1992) 201.
[4] J. McCann, B.N. Ames, Proc. Natl. Acad. Sci. U.S.A. 73 (1975) 950.
[5] P. Cooper, Color in Dyehouse Effluent, Society of Dyers and Colourists, 1995.
[6] W.G. Kuo, Water Res. 26 (1992) 881.
[7] N. Serpone, Solar Energy Materials Solar Cells 38 (1995) 369.
[8] O. Legrini, E. Oliveros, A.M. Braun, Chem. Rev. 93 (1993) 671.
[9] E. Brillas, E. Mur, R. Sauleda, L. Sanchez, J. Peral, X. Domenech, J. Casado, Appl. Catal. B 16 (1998) 31.
[10] M.R. Hoffman, S.T. Martin, W. Choi, D.W. Bahnemann, Chem. Rev. 95 (1995) 69.
[11] C. Dominguez, J. Garcia, M.A. Pedraz, A. Torres, M.A. Galan, Catal. Today 40 (1998) 85.
[12] E. Pelizzetti, C. Minero, Electrochimica Acta 38 (1993) 47.
[13] J.-M. Herrmann, J. Didier, P. Pichat, S. Malato, J. Blanco, Appl. Catal. B 17 (1998) 15.
[14] D.C. Schmelling, K.A. Gray, Water Res. 29 (1995) 2651.
[15] X. Fu, W.A. Zeltner, M.A. Anderson, Appl. Catal. B 6 (1995) 209.
[16] R. Alberici, W.F. Jardim, Appl. Catal. B 14 (1997) 55.
[17] H. Hidaki, J. Zhao, E. Pelizzetti, N. Serpone, J. Phys. Chem. 96 (1992) 2226.
[18] A. Fernandez, G. Lassaletta, V.M. Jimenez, A. Justo, A.R. Gonzalez-Elipe, J.-M. Herrmann, H. Tahiri, Y. Ait-Ichou, Appl. Catal. B 7 (1995) 49.
[19] J.-M. Herrmann, H. Tahiri, Y. Ait-Ichou, G. Lassaletta, A.R. Gonzales-Elipe, A. Fernandez, Appl. Catal. B 13 (1997) 219.
[20] N.J. Peill, M.R. Hoffmann, Environ. Sci. Technol. 29 (1995) 2974.

[21] T. Matsunaga, M. Okochi, Environ. Sci. Technol. 29 (1995) 501.
[22] Y. Xu, C.H. Langford, J. Phys. Chem. 99 (1995) 11501.
[23] C.S. Turchi, D.F. Ollis, J. Catal. 122 (1990) 178.
[24] M.S. Dieckmann, K.A. Gray, Water Res. 30 (1996) 1169.
[25] K. Vinodgopal, D.E. Wynkoop, P.V. Kamat, Environ. Sci. Tchnol. 30 (1996) 1660.
[26] K.E. Karakitsou, X.E. Verykios, J. Catal. 134 (1992) 629.
[27] F. Zhang, J. Zhao, T. Shen, H. Hidaki, E. Pelizzetti, N. Serpone, Appl. Catal. B 15 (1998) 147.
[28] K.E. Karakitsou, X.E. Verykios, J. Phys. Chem. 97 (1993) 1184.
[29] E.C. Akubuiro, X.E. Verykios, J. Phys. Chem. Solids 91 (1989) 17.
[30] T. Ioannides, X.E. Verykios, J. Catal. 145 (1994) 479.
[31] Y.R. Do, W. Lee, K. Dwight, A. Wold, J. Solid State Chem. 108 (1994) 198.
[32] W. Lee, Y.-M. Gao, K. Dwight, A. Wold, Mat. Res. Bull. 27 (1992) 685.